Applied Surface Science 255 (2009) 4149–4152

Contents lists available at ScienceDirect

Applied Surface Science

journal homepage: www.elsevier.com/locate/apsusc

Electrical and photocatalytic properties of $Na_2Ti_6O_{13}$ nanobelts prepared by molten salt synthesis

L. Zhen [a,*], C.Y. Xu [a,b], W.S. Wang [a], C.S. Lao [b], Q. Kuang [b]

[a] School of Materials Science and Engineering, Harbin Institute of Technology, 92 West Dazhi Street, Harbin 150001, China
[b] School of Materials Science and Engineering, Georgia Institute of Technology, Atlanta, GA 30332, USA

ARTICLE INFO

Article history:
Received 13 March 2008
Received in revised form 22 October 2008
Accepted 1 November 2008
Available online 11 November 2008

PACS:
73.40.−c
82.45.Jn
62.23.Hj

Keywords:
Nanomaterials
$Na_2Ti_6O_{13}$
Photocatalytic activity
Electrical property

ABSTRACT

Single-crystalline $Na_2Ti_6O_{13}$ nanobelts were prepared on large-scale by molten salt synthesis at 825 °C for 3 h. The obtained nanobelts have typical width of less than 200 nm and thickness of 10–30 nm, and length up to 10 μm. The growth direction of the nanobelts was determined to be along [0 1 0]. Electrical transport property of an individual nanobelt was measured at room temperature and ambient atmosphere, and results showed that the nanobelts are semiconductor. $Na_2Ti_6O_{13}$ nanobelts exhibited good photocatalytic efficiency for the degradation of RhB under UV irradiation.

1. Introduction

The alkali titanates with a general formula $A_2O{\cdot}nTiO_2$ ($3 \leq n \leq 8$, A = Li, Na, K) exhibit some interesting properties, such as photocatalytic activity and ion conductivity, due to their distinct structures. Titanates with high alkali content ($n = 3$) generally posses a layered structure, while titanates with low alkali content ($n = 4$–8) exhibit tunnel structure although there are some exceptions, such as $K_2Ti_4O_9$ and $Li_2Ti_3O_7$ [1–4]. Among these titanates, alkali hexatitanates with a tunnel structure are suggested to be good photocatalysts. RuO_2-supporting $Na_2Ti_6O_{13}$ shows high photocatalytic activities for water decomposition [5,6]. $Na_2Ti_6O_{13}$ nanorods exhibit good photocatalytic activity for the decomposition of 4-chlorophenol under UV irradiation [7].

Conventionally, $Na_2Ti_6O_{13}$ could be prepared by solid-state reactions from the stoichiometric weights of Na_2CO_3 and TiO_2 or Na_2O and TiO_2. High-temperature calcination above 1100 °C of the mixture of Na_2CO_3 and TiO_2 with molar ratio of 1:6 produces colorless $Na_2Ti_6O_{13}$ needles [3]. $Na_2Ti_6O_{13}$ could be also synthesized by flux growth. Recently, Teshima et al. reported the synthesis of $Na_2Ti_6O_{13}$ whiskers with a diameter of about 2 μm by slow-cooling of a mixture of ($Na_2CO_3 + TiO_2$) in NaCl flux, which was first heated at 1100 °C for 10 h [8,9]. As to the one-dimensional (1D) nanostructures of $Na_2Ti_6O_{13}$, the synthetic approach is mostly limited to hydrothermal synthesis. For example, $Na_2Ti_6O_{13}$ nanobelts were synthesized by hydrothermal treatment of TiO_2 in NaOH aqueous solutions at 130 °C [10]. In the present work, we have synthesized $Na_2Ti_6O_{13}$ nanobelts by molten salt reaction at 825 °C, which is much lower than that for the flux growth of $Na_2Ti_6O_{13}$ whiskers reported by Teshima et al. Large-scale of $Na_2Ti_6O_{13}$ nanobelts with typical width of less than 200 nm and thickness of 10–30 nm, and length up to 10 μm could be prepared by this facile approach. The electrical transport and photocatalytic properties of the synthesized $Na_2Ti_6O_{13}$ nanobelts were measured.

2. Experimental

Single-crystalline $Na_2Ti_6O_{13}$ nanobelts were prepared by molten salt synthesis, which is similar to our previous report except that sodium oxalate was used [11]. All of the chemical reagents are from Sigma Aldrich. In a typical synthesis, 1 mmol $Na_2C_2O_4$ and 6 mmol TiO_2 were mixtured with 2.0 g NaCl and ca. 5 ml surfactant NP-9, and the powders were ground for 20 min. The mixture was placed in a combustion boat and annealed in a

* Corresponding author. Tel.: +86 451 86412133; fax: +86 451 86413922.
E-mail address: lzhen@hit.edu.cn (L. Zhen).

0169-4332/$ – see front matter © 2008 Elsevier B.V. All rights reserved.
doi:10.1016/j.apsusc.2008.11.003

tube furnace at 825 °C for 3 h, and subsequently cooled naturally to room temperature. The resulted products were washed several times with distilled water and then dried at room temperature.

The phase of the obtained product was examined by X-ray diffraction (XRD, Phillips X'-pert). The morphology, structure and dimension of the synthesized $Na_2Ti_6O_{13}$ nanobelts were characterized with scanning electron microscope (SEM, LEO-1530) and transmission electron microscope (TEM, Hitachi HF2000). The nanobelts were first dispersed in ethanol by ultrasonic treatment. Then, one drop of the suspension was transferred to a holey carbon film supported on a copper grid for TEM observation.

The as-synthesized $Na_2Ti_6O_{13}$ nanobelts were dispersed in ethanol and then transferred onto a silicon substrate with predefined Au electrodes. In this way, the nanobelts were lying across the Au electrodes. In order to secure the contact between Au electrodes and nanobelt, Pt layer with thickness of 500 nm was deposited using focused ion beam microscope (FIB, Nova Nanolab 200). Then, the *I–V* characteristic of individual nanobelt was measured at room temperature and ambient atmosphere.

UV–vis absorption spectrometry of the nanobelts solution was measured with a Cary 5000 near-infrared–UV–vis spectrometer. The photocatalytic activity of $Na_2Ti_6O_{13}$ nanobelts was evaluated by measuring the photodegradation of a solution of Rhodamine B (RhB, 1.0×10^{-5} M, 400 ml in a quartz vessel) in the presence of $Na_2Ti_6O_{13}$ nanobelts under exposure to UV light (10 W UV lamp, GPH212T5L/4, Germany). The characteristic absorption of RhB at λ = 553 nm was chosen to monitor the photocatalytic degradation process on UV–vis spectrometer (Schimadzu UV2550).

3. Results and discussion

The general morphology of the obtained nanobelts is shown in Fig. 1a. It was shown that $Na_2Ti_6O_{13}$ nanobelts could be obtained on large-scale by heating a mixture of stoichiometric weights of $Na_2C_2O_4$ and TiO_2 and excess NaCl at 825 °C for 3 h. The belt-like morphology of the obtained product was well documented in the high-magnification SEM image shown in Fig. 1b. $Na_2Ti_6O_{13}$ nanobelts have typical width of less than 200 nm and thickness of 10–30 nm, and length up to 10 μm. Teshima et al. [8] have reported flux growth of $Na_2Ti_6O_{13}$ whiskers with typical diameters of about 2 μm at 1100 °C. It is apparent that the crystal growth of $Na_2Ti_6O_{13}$ is a temperature-dependent behavior. $Na_2Ti_6O_{13}$ nanobelts could be obtained by decreasing the flux growth temperature. The phase of the obtained products was examined by XRD, as shown in Fig. 2. It was shown that phase-pure $Na_2Ti_6O_{13}$ could be obtained by the current molten salt synthesis method at relatively low temperature. No other impurity phase could be detected. $Na_2Ti_6O_{13}$ has a monoclinic structure with space group $C2/m$ and lattice parameters of a = 15.13 Å, b = 3.75 Å, c = 9.16 Å, and β = 99.3° [3]. Fig. 3a shows a typical TEM image of an individual nanobelt with width of about 100 nm, the corresponding electron diffraction pattern is depicted in Fig. 3b. The single-crystalline nature of the synthesized nanobelts was well depicted. The diffraction pattern shown in Fig. 3b was from $[\bar{1}\,0\,1]$ zone axes of $Na_2Ti_6O_{13}$, and the growth direction of $Na_2Ti_6O_{13}$ nanobelts was determined to be along its [0 1 0] crystallographic direction, same as that of $Na_2Ti_6O_{13}$ whiskers [9] and $K_2Ti_6O_{13}$ nanowires [12,13].

UV–vis absorption spectrum of $Na_2Ti_6O_{13}$ nanobelts is shown in Fig. 4. It was shown that the spectrum of $Na_2Ti_6O_{13}$ nanobelts showed strong and wide absorption in the ultraviolet region. The absorption peak is around 314 nm, which is very close to the value of $Na_2Ti_6O_{13}$ whiskers (315 nm) reported by Teshima et al. [9] $Na_2Ti_6O_{13}$ is wide-band semiconductor [9]. *I–V* characters of individual $Na_2Ti_6O_{13}$ nanobelt are depicted in Fig. 5. SEM image of

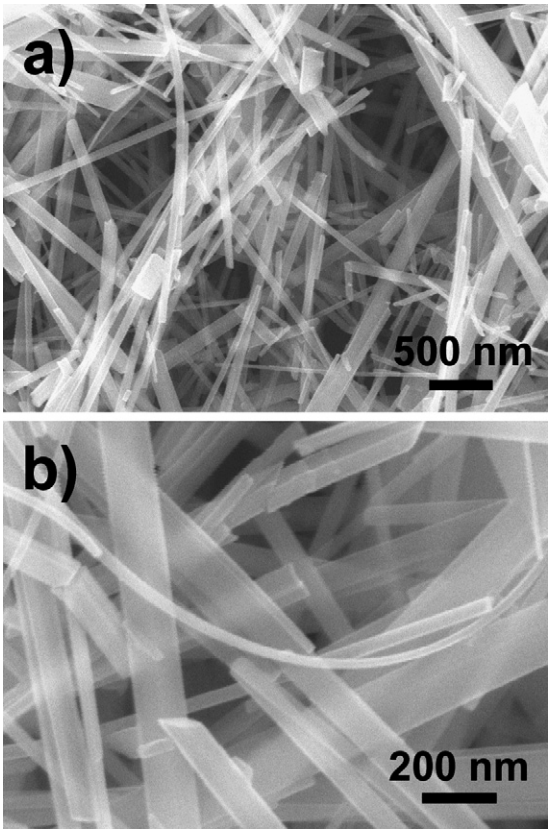

Fig. 1. SEM images of as-synthesized $Na_2Ti_6O_{13}$ nanobelts: (a) low-magnification and (b) high-magnification.

the measured nanobelt aligned between two Au electrodes is shown in the inset of Fig. 5. The good linear relationship between I_{ds} and V_{ds} indicates the Ohmic contact between Au electrodes and the $Na_2Ti_6O_{13}$ nanobelt. The electrical resistance of the measured nanobelt is determined to be $1.38 \times 10^{10}\ \Omega$ by linear fitting the *I–V* curve. The electrical resistivity of a material is expressed by

$$\rho = R\frac{A}{l} \tag{1}$$

where ρ is the electrical resistivity, R the electrical resistance, A the cross-section area, and l the length of the sample. The measured

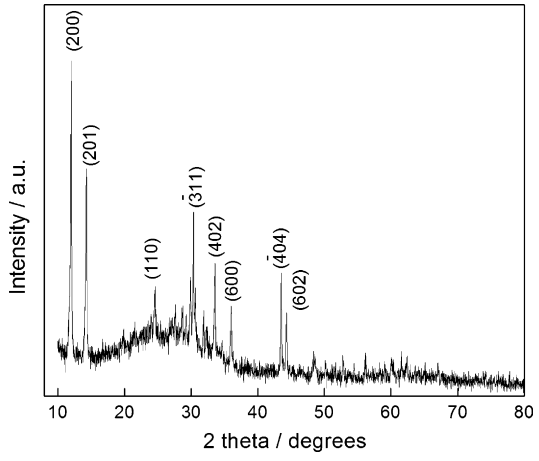

Fig. 2. XRD pattern of as-synthesized $Na_2Ti_6O_{13}$ nanobelts.

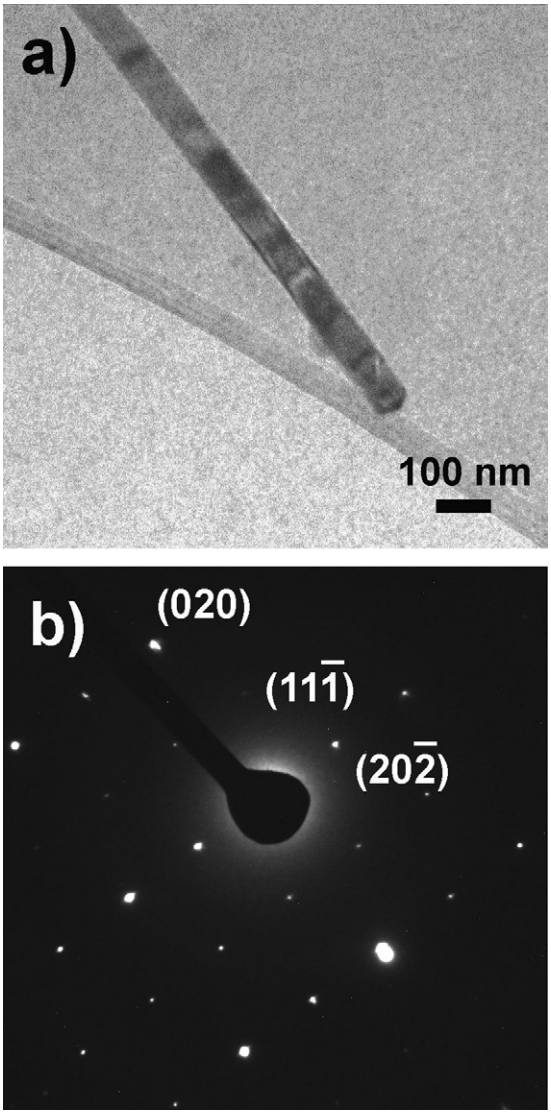

Fig. 3. (a) TEM image of an individual $Na_2Ti_6O_{13}$ nanobelt and (b) its corresponding SAED pattern.

nanobelt has width of 126 nm, and length of 9 μm. Assume the thickness of the nanobelt is 20 nm, the electrical resistivity is calculated to be about 3.86 Ω m, indicating that the $Na_2Ti_6O_{13}$ nanobelt is a semiconductor ceramic.

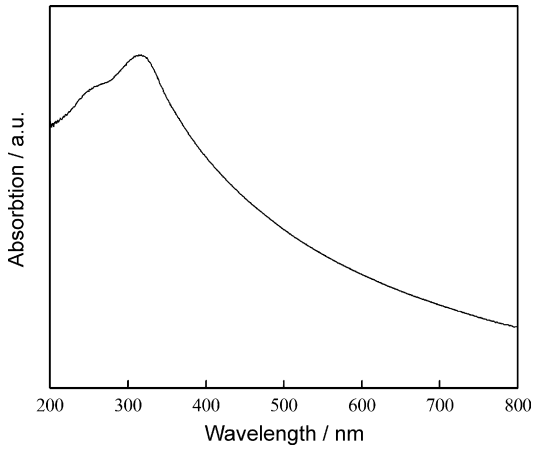

Fig. 4. UV–vis absorption spectrum of $Na_2Ti_6O_{13}$ nanobelts.

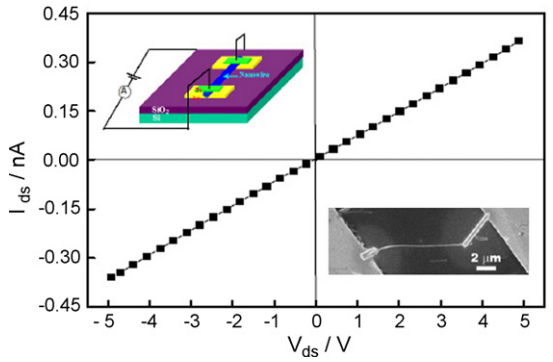

Fig. 5. *I–V* curve of single $Na_2Ti_6O_{13}$ nanobelt with source-drain voltage V_{ds} = 5 V. The upper-left inset is schematic showing the measurement system. The low-right inset is SEM image of the measured nanobelt aligned between two Au electrodes.

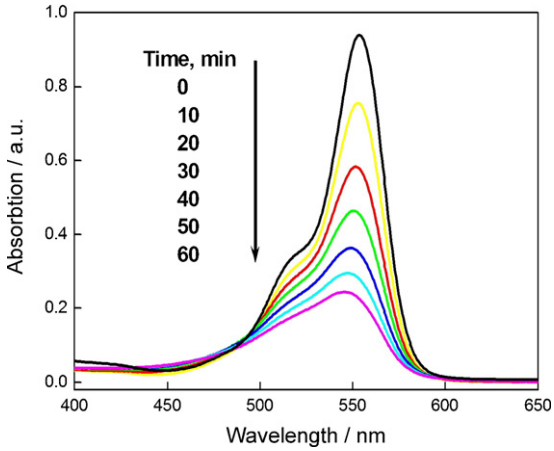

Fig. 6. Absorption spectra of a solution of Rhodamine B (1.0×10^{-5} M, 400 ml) in the presence of 50 mg of $Na_2Ti_6O_{13}$ nanobelts under exposure to UV light.

The photocatalytic activity of $Na_2Ti_6O_{13}$ nanobelts was evaluated by measuring the photodegradation of a solution of RhB (1.0×10^{-5} M, 400 ml in a quartz vessel) in the presence of 50 mg nanobelts under exposure to UV light (10 W UV lamp, GPH212T5L/4, Germany) at room temperature and ambient atmosphere. The characteristic absorption peak of RhB at λ = 553 nm was chosen to evaluate the photocatalytic degradation process on UV–vis spectrometer. Fig. 6 shows the evolution of RhB absorbance spectra in the presence of $Na_2Ti_6O_{13}$ nanobelts exposed to UV light for various time periods. The absorption peak value at λ = 553 nm decreases sharply as the UV light exposure time increases, and the photodegradation efficiency reaches 76% after 60 min of reaction. No new absorption bands appear in the spectrum, indicating the photocatalytic degradation of RhB during the process. The photocatalytic degradation of RhB by $Na_2Ti_6O_{13}$ nanobelts with UV irradiation follows the pseudo-first-order reation:

$$\ln\left(\frac{C_0}{C}\right) = kt \quad (2)$$

where k is the apparent photodegradation rate constant, which is 0.02394 min^{-1} in this experiment. $Na_2Ti_6O_{13}$ with a rectangular tunnel structure has high efficiency to produce photoexcited charges (electrons and holes) [6], which is thought to be associated with its high photocatalytic activity.

4. Conclusions

We have successfully prepared photocatalytic $Na_2Ti_6O_{13}$ nanobelts on large-scale via molten salt synthesis. The synthesized nanobelts are single-crystalline with a preferential growth direction of [0 1 0]. Electrical transport measurement of individual nanobelt shows that the nanobelt is a semiconductor. $Na_2Ti_6O_{13}$ nanobelts are good photocatalytic for the degradation of RhB under UV irradiation.

Acknowledgements

The author (C.Y. Xu) thank Prof. Z.L. Wang for his kind permission to use facilities at Georgia Tech., and Y.-F. Lin for fruitful discussion. C.Y. Xu was supported by the Development Program for Outstanding Young Teachers and Internationalization Foundation of HIT.

References

[1] S. Andersson, A.D. Wadsley, Acta Crystallogr. 14 (1961) 1245.
[2] J. Akimoto, H. Takei, J. Solid State Chem. 83 (1989) 132.
[3] S. Andersson, A.D. Wadsley, Acta Crystallogr. 15 (1962) 194.
[4] T. Sasaki, Y. Fujiki, J. Solid State Chem. 83 (1989) 132.
[5] Y. Inoue, T. Kubokawa, K. Sato, J. Chem. Soc., Chem. Commun. (1990) 1298.
[6] S. Ogura, M. Kohno, K. Sato, Y. Inoue, Appl. Surf. Sci. 121/122 (1997) 521.
[7] V. Štengl, S. Bakardjieva, J. Šubrt, E. Večernková, L. Szatmary, M. Klementová, V. Balek, Appl. Catal. B 63 (2006) 20.
[8] K. Teshima, K. Yubuta, T. Shimodaira, T. Suzuki, M. Endo, T. Shishido, S. Oishi, Cryst. Growth Des. 8 (2008) 465.
[9] K. Teshima, K. Yubuta, S. Sugiura, T. Suzuki, T. Shishido, S. Oishi, Bull. Chem. Soc. Jpn. 79 (2006) 1725.
[10] R.A. Zárate, S. Fuentes, J.P. Wiff, V.M. Fuenzalida, A.L. Cabrera, J. Phys. Chem. Solids 68 (2007) 628.
[11] C.Y. Xu, Q. Zhang, H. Zhang, L. Zhen, J. Tang, L.-C. Qin, J. Am. Chem. Soc. 127 (2005) 11584.
[12] G.H. Du, Q. Chen, P.D. Han, Y. Yu, L.-M. Peng, Phys. Rev. B 67 (2003) 035323.
[13] R.H. Wang, Q. Chen, B.L. Wang, S. Zhang, L.-M. Peng, Appl. Phys. Lett. 86 (2005) 133101.